74N16619

NASA TECHNICAL NOTE
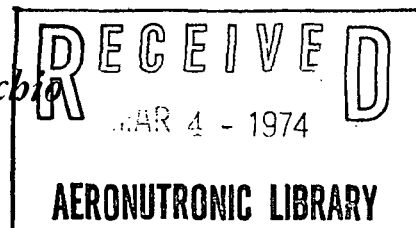
NASA TN D-7553

FORCED-CONVECTION PEAK HEAT FLUX
ON CYLINDRICAL HEATERS IN
WATER AND REFRIGERANT 113

by Thomas H. Cochran and Charles R. Andracchio

Lewis Research Center
Cleveland, Ohio 44135

NATIONAL AERONAUTICS AND SPACE ADMINISTRATION • WASHINGTON, D. C. • FEBRUARY 1974

1. Report No. NASA D-7553	2. Government Accession No.	3. Recipient's Catalog No.		
4. Title and Subtitle FORCED-CONVECTION PEAK HEAT FLUX ON CYLINDRICAL HEATERS IN WATER AND REFRIGERANT 113		5. Report Date February 1974		
		6. Performing Organization Code		
7. Author(s) Thomas H. Cochran and Charles R. Andracchio		8. Performing Organization Report No. E-7659		
9. Performing Organization Name and Address Lewis Research Center National Aeronautics and Space Administration Cleveland, Ohio 44135		10. Work Unit No. 502-24		
		11. Contract or Grant No.		
12. Sponsoring Agency Name and Address National Aeronautics and Space Administration Washington, D. C. 20546		13. Type of Report and Period Covered Technical Note		
		14. Sponsoring Agency Code		
15. Supplementary Notes				

16. Abstract

An investigation was conducted of the peak heat flux on cylindrical heaters in a fluid flowing perpendicular to the major axis of the heater. The test fluids were water and Refrigerant 113. Heaters of 0.049 to 0.181 cm diameter were tested over a fluid velocity range of 10.1 to 81.1 cm/sec. The experimental results were observed to fall within two regions based on the vapor removal geometry: jets or sheets. Mathematical models for each region successfully correlated the data for both fluids.

17. Key Words (Suggested by Author(s)) Boiling Two-phase flow Fluid mechanics Heat transfer		18. Distribution Statement Unclassified - unlimited Cat. 33		
19. Security Classif. (of this report) Unclassified	20. Security Classif. (of this page) Unclassified		21. No. of Pages 21	22. Price* $2.75

FORCED-CONVECTION PEAK HEAT FLUX ON CYLINDRICAL

HEATERS IN WATER AND REFRIGERANT 113

by Thomas H. Cochran and Charles R. Andracchio

Lewis Research Center

SUMMARY

An investigation was conducted of the peak heat flux on cylindrical heaters in a fluid flowing perpendicular to the major axis of the heater. The test fluids were water and Refrigerant 113. Heaters of 0.049 to 0.181 centimeter diameter were tested over a fluid velocity range of 10.1 to 81.1 centimeters per second. The experimental results were observed to fall within two regions based on the vapor removal geometry: jets or sheets. The data in the jet region were successfully correlated by a mathematical model based on the superposition of a pool boiling prediction and a contribution due to single-phase forced convection. The sheet region data substantiated a previously published theory which predicted the peak heat flux as a function of fluid velocity and heater size.

INTRODUCTION

The process of boiling has become of increasing interest in recent years because of the desire to transfer large quantities of heat in devices such as power generators and spacecraft. A primary design consideration when equipment is selected to operate in a boiling environment is termed the burnout or peak heat flux. This critical point separates the nucleate and film boiling regions, the latter of which is generally characterized by prohibitively high surface temperatures. Therefore, it is important to be able to accurately predict the peak heat flux in order to insure efficient and safe design.

Work that has been done on the burnout heat flux can be categorized into two general groupings, (1) pool boiling and (2) forced convection. Lienhard and Dhir (ref. 1) have reported the most recent research on pool boiling burnout. In addition to summarizing the myriad of data available in the field, they investigated the effects of fluid properties, geometry, and gravity level. A primary result of this work is a correlation of the burnout heat flux as a function of the Bond number, which is the ratio of gravity to surface tension effects.

Forced convection burnout can be classified depending on whether the process is occurring on an internal or external surface. The former, primarily involving flow in pipes, has been studied by numerous investigators and a great deal of information is available in the literature. However, the latter topic has received comparatively little attention, the main contributions being those of Vliet and Leppert (ref. 2) and McKee (ref. 3).

Vliet and Leppert investigated the burnout of cylindrical heaters in saturated distilled water. The heaters were oriented so that they were perpendicular to the flow. This condition is termed crossflow. Stainless-steel wires and tubes of 0.0254 to 0.48 centimeter diameter were tested over a fluid velocity range of 36.6 to 289.8 centimeters per second. The obtained peak heat flux data was successfully correlated as a function of fluid velocity and size.

McKee also conducted experiments with cylindrical heaters in nearly saturated water flowing perpendicular to the main axis of the cylinders. The heaters ranged from 0.64 to 1.78 centimeters in diameter while the flow velocity was varied from 104.3 to 165.9 centimeters per second. Although McKee found the same trends in the results with respect to size and velocity as did Vliet and Leppert, the latter's correlation did not fit the data.

The aforementioned work has been significant in developing a general understanding of forced convection burnout. However, the entire range of interest insofar as flow conditions and fluid properties is concerned has not been explored. For instance, the validity of the correlation of Vliet and Leppert must be highly suspect at low velocities since it predicts a zero burnout heat flux at zero velocity. (One would expect a transition to a pool boiling prediction, such as Lienhard's, as the liquid velocity is decreased.) Lastly, all the work has been conducted with water while the fluids of interest in spacecraft, for instance, may be cryogens which have much lower peak heat fluxes than water.

The purpose of the current work was to study the burnout of cylindrical heaters in the crossflow of a saturated liquid as a function of free stream velocity. The heater sizes chosen, 0.049 to 0.181 centimeter diameter, were in the low Bond number range, thus simulating the heat transfer characteristics larger heaters would experience in the low gravity environment of space. Tests were conducted with distilled water at relatively high flows, up to 81.1 centimeters per second, in order to provide an independent verification of the correlation of Vliet and Leppert. Low velocity data, down to 14.6 centimeters per second, were taken in order to investigate the transition between Vliet and Leppert's flowing model and Lienhard's pool boiling model. A series of tests were also conducted with Refrigerant 113 because of its characteristically low maximum heat flux. The majority of the experimental data was obtained from gauges; however, 16 millimeter high-speed motion pictures were taken of the liquid and vapor flow patterns for selected test runs.

SYMBOLS

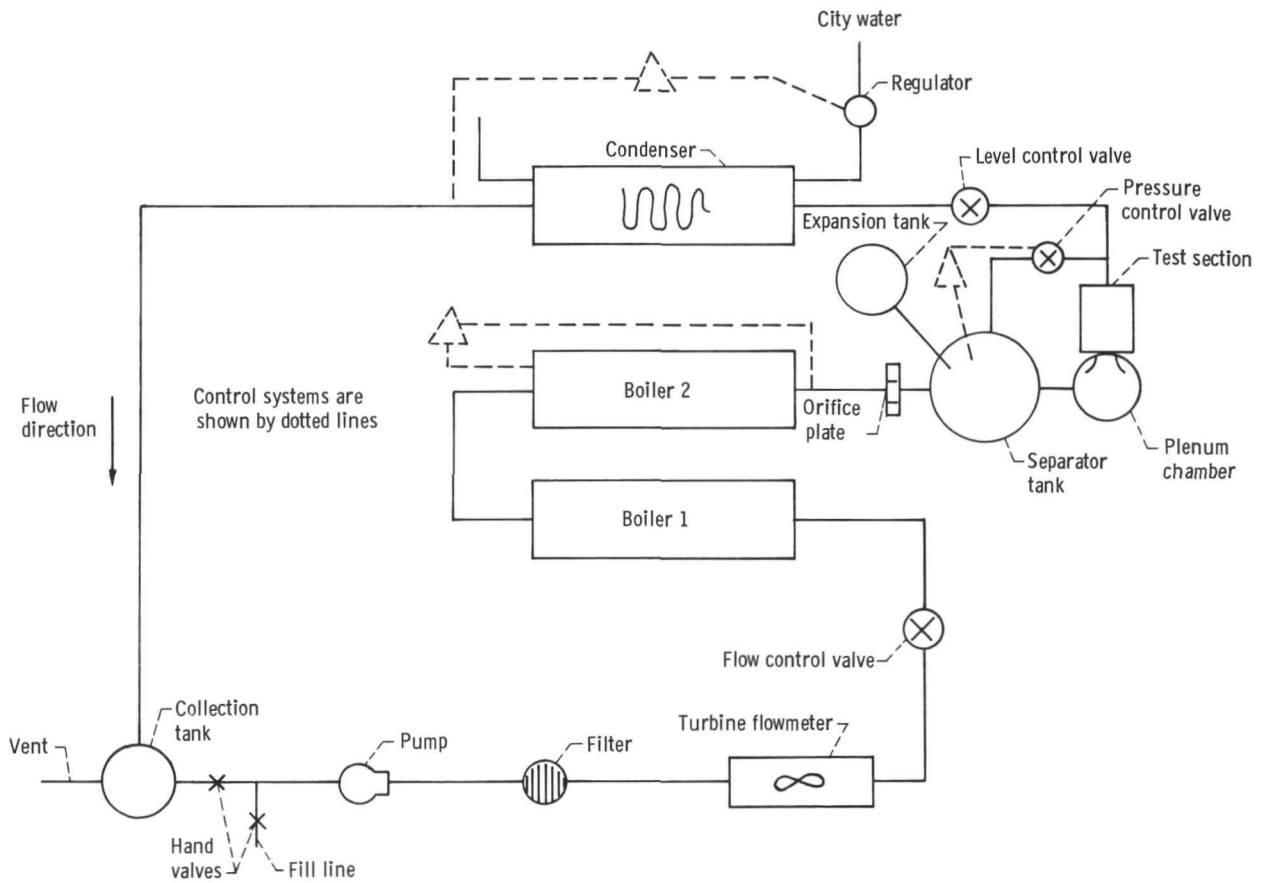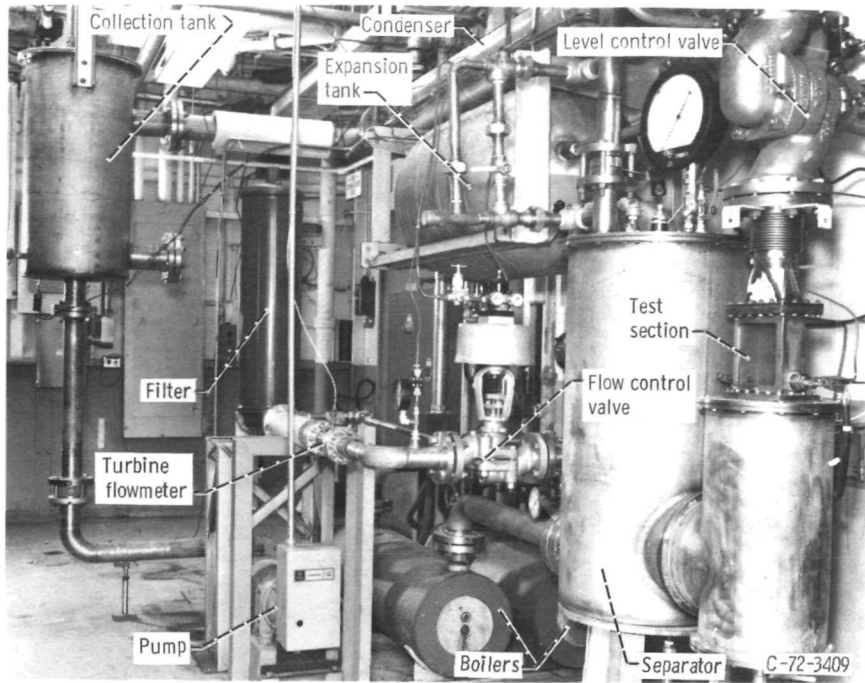|	
B	variable in low flow rate model for q_{max}, $W^{1/2}/m$
B_o	Bond number, $R^2 g(\rho_f - \rho_g)/\sigma$, dimensionless
C_p	constant pressure specific heat, $J/(kg)(K)$
C_1	correlation constant for q_{max} as a function of ΔT_{sat}, $W/(m^2)(K^2)$
D	heater diameter, cm
$\overline{f}$	angle average value of fraction of surface heat flux which goes into production of vapor, dimensionless
g	acceleration of gravity, cm/sec^2
$\overline{h}_c$	heat transfer coefficient, $W/(m^2)(K)$
h_{fg}	latent heat of vaporization, J/kg
K	thermal conductivity, $W/(m)(K)$
q	heat flux, W/m^2
q_c	heat flux due to single-phase convection, W/m^2
q_{max}	forced convection burnout heat flux, W/m^2
q_{PB}	pool boiling burnout heat flux, W/m^2
q_z	pool boiling burnout heat flux on infinite flat plate, W/m^2
R	heater radius, cm
T_{sat}	saturation temperature, K
ΔT_{sat}	$T_{wall} - T_{sat}$, K
T_{wall}	wall temperature, K
V	average free stream velocity, cm/sec
α	thermal diffusivity, m^2/sec
μ	dynamic viscosity, $kg/(m)(sec)$
ν	kinematic viscosity, m^2/sec
ρ_f	liquid density, kg/m^3
ρ_g	vapor density, kg/m^3
σ	surface tension, dynes/cm

Figure 1. – Experimental apparatus.

APPARATUS AND PROCEDURE

Experimental Apparatus

The experimental apparatus shown in figure 1 is basically a closed-loop flow system which provided a flow of saturated test liquid perpendicular to a heating wire inside the test section of the loop. The test fluid was pumped from the collection tank through a filter, a turbine flowmeter, a flow control valve, and into the system's boilers. From the boilers the fluid progressed through an orifice plate, a liquid-vapor separator tank, the test section, a condenser, and returned to the collection tank. An expansion tank coupled to the liquid-vapor separator was used to reduce pressure surges and provide stability of flow, particularly during the initial boiling of the test liquid in the system's boilers. Maintaining the liquid-vapor level in the separator tank slightly above the test heater assured the arrival of nearly saturated liquid at the heating wire.

Flow rates were measured by the turbine flowmeter calibrated for the specific fluid used in the system. Maximum flow rate capability of the system was 5050 cubic centimeters per second for water and 4420 cubic centimeters per second for Refrigerant 113. Thermocouples were located at various points throughout the system.

Automatic controllers were located at several positions in the loop to facilitate steady-state operation of the system (fig. 1). One unit regulated power to one of the boilers by sensing its outlet water temperature. The second boiler was manually controlled. Another controller maintained the pressure in the separator tank at 1.38×10^4 newtons per square meter above atmospheric pressure by periodically bleeding off vapor to a point downstream of the test section. The third unit controlled the flow of city water through the condenser by sensing the temperature of the test fluid leaving the condenser. All of these controllers were set to operate such that a steady flow of nearly saturated fluid was delivered to the test section.

The experimental test section shown in figure 2 was a rectangularly shaped flow channel with a transparent plastic window on the front surface. Cross-sectional dimensions of the flow channel were 12.70 by 5.08 centimeters. The plastic window was pressed against an O-ring seal by a flange in such a manner as to make the inner surface of the window flush with the front wall of the flow section. When assembled, a viewing area of 12.7 by 13.6 centimeters was available. A bell-shaped plenum chamber below the test section was used to provide a smooth flow of liquid into the channel.

A typical heating wire shown in figure 3 was located approximately 11.8 centimeters above the entrance to the flow channel. The heating elements were 10.16-centimeter-long Nichrome wires fastened to two copper leads. The copper leads were inserted through the sides of the test section positioning the heater wire in the center of the flow.
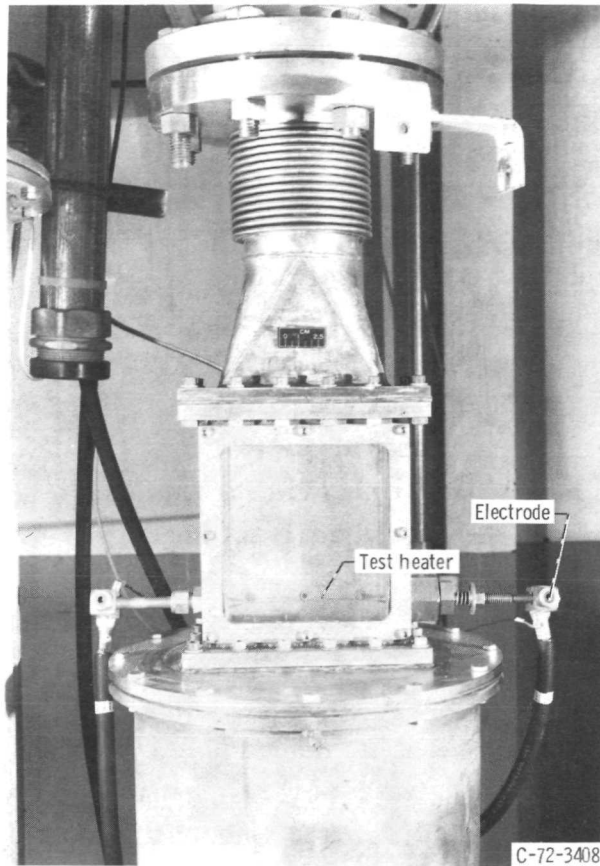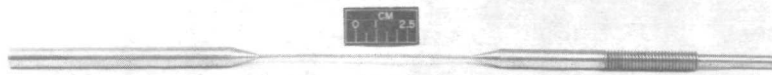
Figure 2. – Experimental test section.

Figure 3. – Experimental heater.

The Nichrome wires used in the tests ranged from 0.049 to 0.181 centimeter in diameter. Before placing the heater in the test section, it was washed with soap and water and then rinsed with acetone.

Procedure

After filling the system with the required test liquid, flow was started and manually controlled until a steady-state flow rate was achieved. Power to the boilers was then

applied and the controllers were preset to the desired operating conditions. When the system neared the temperature and pressure of the test conditions, the controllers were activated; the system was then operated automatically until a steady state was reached.

Power to the heating wire was applied in small increments, while the current was monitored. During each increment the flow conditions past the wire were visually observed and in some cases photographed. As the heat flux increased, the various phases of boiling were clearly distinguished. When burnout occurred, the monitored current changed drastically. The current at burnout and wire resistance were used to calculate the peak heat flux. Values for resistance were obtained from manufacturers' specifications at room temperature. The errors involved in correcting for wire size and temperature were negligible.

Flow Field Measurements

Measurements of the liquid velocity as a function of position were made at the heater position to ensure that the velocity was relatively constant. In addition, the measurements were used to verify the assumption that the velocity profile across the channel was flat.

Velocity was measured using a quartz coated cylindrical hot film anemometer which was set to operate with a 5.5° C overheat. Data were taken at both high and low flow rates for both test fluids after the system had been brought up to test temperature and was stable. Prior to making the velocity surveys, the sensor was calibrated by recording the sensor output over a range of flow rates with the probe positioned in the center of the channel. The velocity assumed at that position was the average value computed from the volumetric flow rate. This assumption was verified by data which showed that the profiles were flat and that the boundary layer was very small (< 0.1 cm for water). The results of the two water surveys are shown in figure 4 for 5200 and 1300 cubic centimeters per second. As can be seen, the average value of velocity as a function of position was within ±5 percent of the center value with the exception of one data point at the highest flow rate which was 7 percent high. The variation in velocity due to the pressure oscillations was also small, the maximum deviation from the center value being less than ±5 percent at the low flow rate and ±7 percent at the high flow rate. Similar results were obtained for Refrigerant 113.
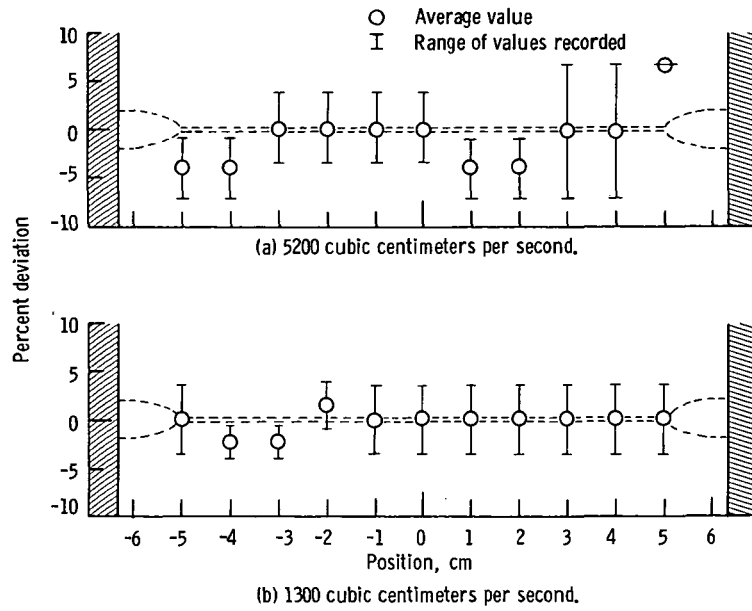
Figure 4. - Percent deviation of velocity from centerline velocity for water.

TABLE I. - SUMMARY OF WATER DATA

| Run number	Wire diameter, cm	Liquid temperature, °C	Subcooling temperature, °C	Velocity, cm/sec	Burnout heat flux, W/m²
1	0.080	103.6	- .4	37.5	260×10⁴
2	.080	103.4	- .2	28.4	190
3	.050	103.3	- .3	37.5	291
4	.112	103.7	- .2	37.5	200
5	.112	103.5	- .1	28.4	172
6	.112	103.7	- .3	45.8	220
7	.080	103.8	- .3	45.8	297
8	.049	103.5	- .1	26.2	179
9	.049	103.7	- .3	45.8	368
10	.051	103.4	- .1	22.0	191
11	.082	103.6	- .3	22.0	200
12	.082	103.2	0	14.6	169
13	.051	103.2	.1	14.6	174
14	.114	103.0	- .2	22.0	178
15	.114	103.0	.2	14.6	179
16	.051	103.8	- .1	60.4	348
17	.051	103.8	- .1	70.4	328
18	.081	103.7	.1	60.4	273
19	.081	103.6	0	70.4	343
20	.116	103.6	.1	60.4	334
21	.116	103.7	- .1	70.4	384
22	.051	103.4	- .2	81.1	296
23	.081	103.5	- .2	80.5	387
24	.116	103.3	- .1	80.5	421
25	.051	103.6	.1	70.4	349
26	.051	103.2	.1	80.4	296

8
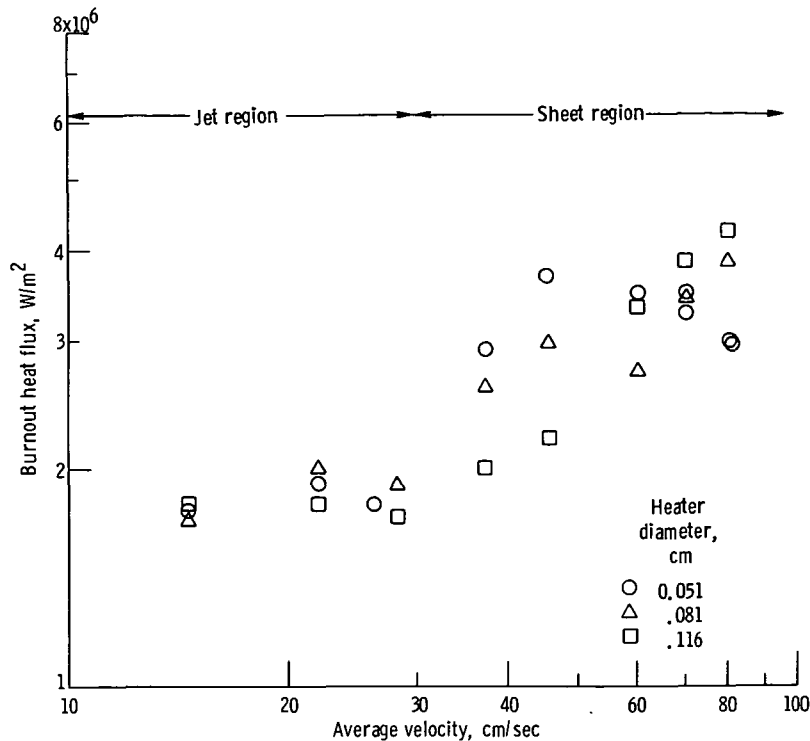
Figure 5. - Burnout heat flux as a function of velocity for water.

RESULTS AND DISCUSSION

Experimental Results

Water. - The burnout process with this test liquid was a highly localized process. A small section of the heater first glowed red and then melted to destruction.

A summary of the water data and test conditions is presented in table I. A plot of the burnout heat flux as a function of average liquid velocity is shown in figure 5 for the three different heaters. It can be seen that the burnout heat flux at first increases slowly with velocity. Above 30 centimeters per second, however, the burnout point increases at a relatively rapid rate up to values at 80 centimeters per second that are as much as two and a half times greater than those at 15 centimeters per second. There was no obvious systematic effect of heater size in the data.

The two largest heaters tested generally indicate an increase in burnout heat flux as velocity was increased. The 0.051 centimeter-diameter heater also behaved in the same manner up to a velocity of about 46 centimeters per second. However, at higher velocities there was a distinct decrease in the burnout heat flux. In order to verify this trend in the data, two of the higher velocity runs were repeated. They yielded the same results. The reason for this behavior could not be determined.

9
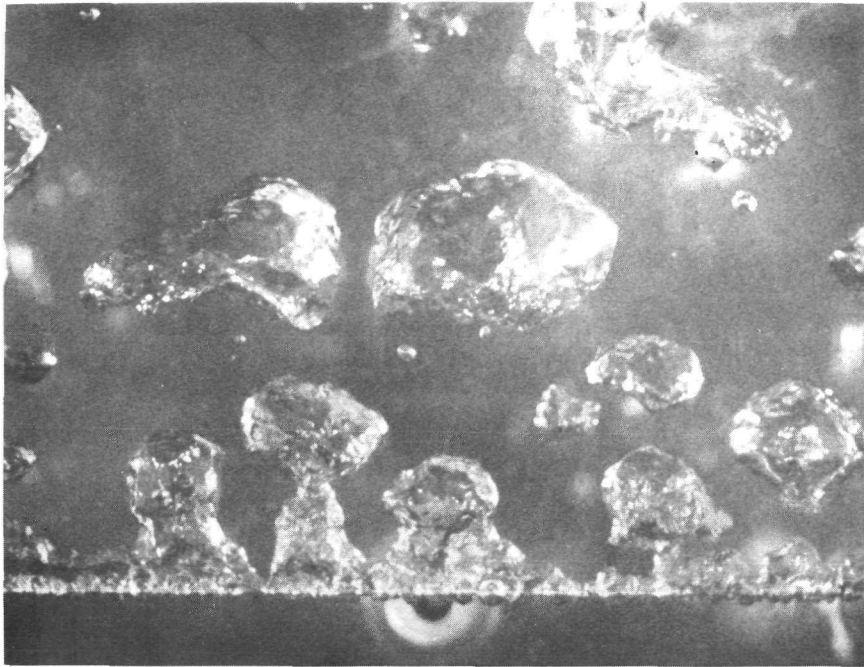
(a) 0.051-Centimeter-diameter heater; 14.6 centimeters per second.
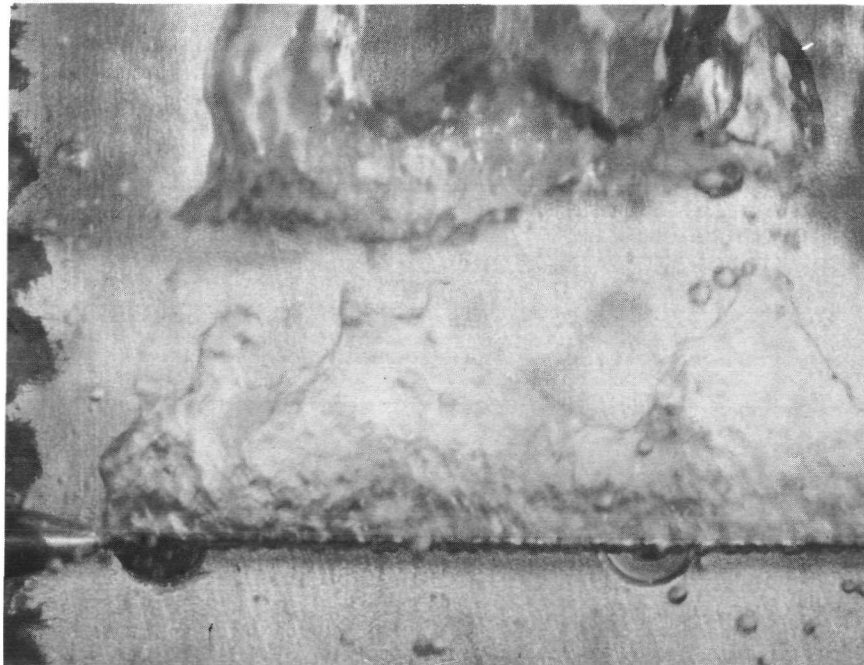
(b) 0.116-Centimeter-diameter heater; 60.4 centimeters per second.

Figure 6. – Water boiling at heat flux just below burnout.

A better understanding of the burnout processes was obtained from the high-speed motion pictures. Figure 6(a) shows the 0.051-centimeter-diameter heater with water flowing at 14.6 centimeters per second just before burnout occurred. The vapor removal patterns were very similar to those that occur in a pool boiling situation, that is, there were regularly spaced jets of vapor separated by columns of liquid. A relatively high velocity run, 60.4 centimeters per second, is shown in figure 6(b) for the 0.116-centimeter-diameter heater. The photograph indicates a large continuous vapor cavity behind the heater. Periodically, long sheets of vapor were torn from this cavity. This is identical to what Vliet and Leppert observed in their experiments.

It is apparent from both the peak heat flux measurements and the high-speed motion pictures that the mechanisms responsible for causing burnout were different at low liquid velocities than at high liquid velocities. Accordingly, the data were separated into two regions as shown in figure 5. These regions were labeled the jet region and the sheet region as a consequence of the observed vapor removal patterns.

Refrigerant 113. - The tests with the Refrigerant 113 were much easier to conduct because of its relatively low peak flux (approximately an order of magnitude lower than that for water.) As a consequence, when burnout occurred the heater was not destroyed but started to glow red. This usually occurred in the center of the heater first and then spread along its entire length.

A summary of the data and test conditions for this liquid is presented in table II.

TABLE II. - SUMMARY OF REFRIGERANT 113 DATA

| Run number	Wire diameter, cm	Liquid temperature, ^{o}C	Subcooling temperature, ^{o}C	Average velocity, cm/sec	Burnout heat flux, W/m^2
1	0.116	53.2	3.0	20.1	24.0×10^4
2	.116	53.3	2.9	30.2	26.1
3	.116	53.3	2.9	40.3	27.0
4	.116	52.9	3.3	50.3	28.2
5	.116	52.8	3.4	60.4	29.4
6	.116	52.9	3.3	70.4	30.0
7	.181	53.0	3.1	10.1	23.1
8	.181	53.2	2.9	20.1	21.5
9	.181	53.3	2.9	30.2	25.6
10	.181	53.3	2.9	40.3	25.6
11	.181	52.9	3.2	50.3	26.4
12	.181	52.9	3.3	60.4	27.3
13	.181	52.8	3.3	70.4	28.2
14	.051	53.0	3.0	10.1	29.8
15	.051	53.0	3.0	20.1	30.7
16	.051	53.2	2.8	30.2	33.8
17	.051	53.3	2.8	40.3	35.0
18	.051	52.9	3.0	50.3	37.0
19	.051	53.0	3.1	60.4	38.2
20	.051	53.0	3.1	70.4	41.0
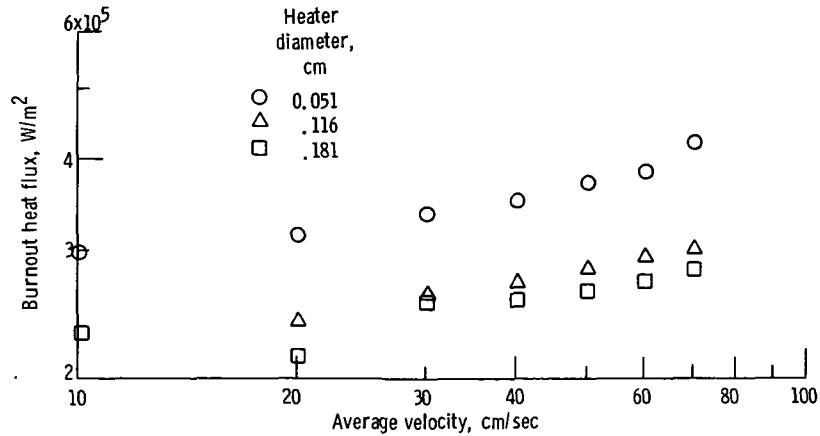
Figure 7. - Burnout heat flux as a function of velocity for refrigerant 113.

The burnout heat flux is plotted as a function of velocity in figure 7. It is apparent that the peak heat flux increased relatively slowly over the entire velocity range. In contrast to the water data, there is also a decided heater size effect; the smallest heater exhibiting the highest burnout heat flux for a given liquid velocity.

Examination of the high-speed motion pictures revealed similarities between the Refrigerant 113 data and the low velocity water results. Typical photographs for Refrigerant 113 at two liquid velocities are shown in figure 8. It is apparent from these pictures that the vapor removal processes for Refrigerant 113 for the low as well as the high velocity tests resemble a jetting phenomena. Although a vapor cavity was present behind the heater, as there was in the high velocity water data, it was much smaller than the cavity seen in the water tests and there was no evidence of long sheets of vapor being torn away from the cavity.

Analytical Predictions

Pool boiling burnout. - The burnout of cylindrical heaters in a pool has been developed by Lienhard in reference 1. The model is based on the hydrodynamic instability of jets of vapor and columns of liquid on the heater surface. The derived relation for Bond numbers between approximately 0.01 and 1 is

$$q_{PB} = \frac{0.94 \, q_z}{(B_o)^{1/8}} \tag{1}$$

(a) 0.181-Centimeter-diameter heater; 30.2 centimeters per second.

(b) 0.051-Centimeter-diameter heater; 70.4 centimeters per second.

Figure 8. – Refrigerant 113 boiling at heat flux just below burnout.

with q_z the burnout heat flux on an infinite flat plate, as derived by Zuber (ref. 4), expressed as

$$q_z = \left(\frac{\pi}{24}\right) \rho_g^{1/2} h_{fg} \left[6g \left(\rho_f - \rho_g\right)\right]^{1/4} \qquad (2)$$

and

$$B_0 = R^2 \frac{g(\rho_f - \rho_g)}{\sigma} \qquad (3)$$

Forced convection burnout - jet model. - The water data taken at the lower flow rates as well as all the Refrigerant 113 data indicate that the burnout heat flux was increasing at a relatively slow rate as the average free stream velocity became larger. The motion pictures also revealed that the vapor removal processes under these conditions resembled the familar jetting phenomena seen in pool boiling burnout. A mathematical model to predict the burnout point under these conditions must, therefore, be consistent with these observations together with the requirement that it degenerate to the pool boiling value at zero velocity.

A method which has been attributed to Gambill (ref. 5), adds a convective heat flux, q_c to the pool boiling heat flux, q_{PB}, to obtain the burnout point under forced convection conditions, or

$$q_{max} = q_{PB} + q_c \qquad (4)$$

The convective heat flux is defined by

$$q_c = \bar{h}_c \, \Delta T_{sat} \qquad (5)$$

The heat transfer coefficient $\bar{h}_c$, from Krieth (ref. 6), is

$$\bar{h}_c = 0.676 \, \frac{K}{D} \left(\frac{V_\infty D}{\nu}\right)^{0.466} \left(\frac{\mu C_p}{K}\right)^{0.31} \qquad (6)$$

14

A relation between q and ΔT_{sat} for a forced convection boiling situation has been proposed by Forster and Grief (ref. 7) to be of the form

$$q = C_1 (\Delta T_{sat})^2 \qquad (7)$$

Vliet and Leppert verified this dependence with experimental data and found C_1 to equal 38.6×10^2 W/$(m^2)(K^2)$ for water. Data for forced convection boiling of Refrigerant 113 is not available and, therefore, a value for C_1 must be assumed. There is data in the literature (ref. 8) for pool boiling of water and Refrigerant 113 from the identical surface. In addition, the pool boiling burnout heat flux can be calculated for both fluids from equation (1). Therefore, as an estimate for $(C_1)_{113}$, the following relation is assumed:

$$(C_1)_{113} = (C_1)_{water} \left(\frac{q_{113}}{q_{water}} \right) \qquad (8)$$

where the heat flux ratio on the right side of the equation is a pool boiling value for either nuclear boiling or the peak heat flux at a given temperature difference ΔT_{sat}. Use of the correlations developed in reference 8 results in $(C_1)_{113} = 22.30 \times 10^2$. Insertion of the burnout heat fluxes, computed from equation (1), into equation (8) results in $(C_1)_{113} = 6.6 \times 10^2$. The average value of 14.46×10^2 will be used in this analysis.

Combining equations (4), (5), and (7) with q set equal to q_{max} results in a solution of the form

$$q_{max} = \frac{1}{2} \left(B^2 + 2q_{PB} + B \sqrt{B^2 + 4q_{PB}} \right) \qquad (9)$$

where

$$B = \bar{h}_c \left(\frac{1}{C_1} \right)^{1/2} \qquad (10)$$

Forced convection burnout - sheet model. - Vliet and Leppert's model is based on a deficiency of liquid in the two-phase mixture at the rear portion of the heater. Their derived relation for q_{max} is

$$q_{max} = \text{Constant x} \left(\frac{K \, \Delta T_{sat}}{\bar{f}} \right) \left(\frac{V_\infty}{D\alpha} \right)^{1/2} \tag{11}$$

All of the terms in the equation can be evaluated directly except the temperature difference ΔT_{sat} and $\bar{f}$, the angle averaged value of the fraction of surface heat flux which goes to the production of vapor. The ΔT_{sat} term was disposed of by using equation (7) with q set equal to q_{max}. This left only $\bar{f}$ to be determined from their experimental data. The equation which correlated their results is

$$q_{max} = 30.8 \times 10^4 \, \frac{V_\infty^{1/2}}{D^{0.15}} \tag{12}$$

This requires that

$$\bar{f} = 0.054 \, \frac{V_\infty^{0.25}}{D^{0.42}} \tag{13}$$

In order to apply this model to Refrigerant 113, equation (7) (with $(C_1)_{113}$ set equal to 14.46×10^2) and equation (13) were inserted into equation (11). The resulting expression is

$$q_{max} = 2.45 \times 10^4 \, \frac{V_\infty^{1/2}}{D^{0.15}} \tag{14}$$

It must be mentioned that the use of equation (13) for $\bar{f}$ in this derivation is not straight-forward. Vliet and Leppert indicate that $\bar{f}$ is a function of fluid properties, among other things, and equation (13) was obtained for water. However, because of the lack of data for Refrigerant 113, or any other fluid for that matter, equation (13) is the only relation available. The validity of the use of this expression will be discussed later in this report. The fluid properties used in the calculations are presented in table III.

16

TABLE III. - FLUID PROPERTIES[a]

Parameter	Water	Refrigerant 113
Constant pressure specific heat, C_p, J/(kg)(K)	4.23×10^4	9.62×10^3
Latent heat of vaporization, h_{fg}, J/kg	2.24×10^5	0.145×10^5
Thermal conductivity, K, W/(m)(K)	6.83	0.578
Liquid density, ρ_f, kg/m^3	9.56	1495
Vapor density, ρ_g, kg/m^3	0.592	0.885
Surface tension, σ, dynes/cm	51	15.2
Kinematic viscosity, ν, m^{2}sec	2.92×10^{-7}	2.08×10^{-7}
Dynamic viscosity, μ, kg/(m)(sec)	2.79×10^{-4}	3.11×10^{-4}
Thermal diffusivity, α, m^2/sec	17×10^{-8}	4.03×10^{-8}

[a]Properties evaluated at 103° C for water and 53.5° C for Refrigerant 113.

Discussion of Results

The models were evaluated for both water and Refrigerant 113 and the results are presented in figure 9. All of the experimental data are shown with the exception of the previously discussed high flow rate water points for the 0.051 centimeter heater. Equation (12) correlates the high flow rate water data very nicely. The maximum deviation of the data from the prediction is about 20 percent. This is normal scatter for boiling experiments. At low flow rates equation (9), evaluated for the three heater sizes, brackets the data. It is apparent from this figure that equation (9) clearly predicts the trends in the water data as a function of velocity for low flow rates. The scatter in this data is no worse than what other workers have experienced.

Considering now the Refrigerant 113 data, it can be seen that equation (9) predicts the trends in the data in so far as both velocity and size are concerned. A check on the assumed value of $(C_1)_{113}$ was made by determining the least-squares curve fit to the data in terms of $(C_1)_{113}$. The value of $(C_1)_{113}$ which resulted in the best fit was 5.86×10^2 W/(m^2)(K^2). This indicates that, at least from an order of magnitude point of view, the value assumed for $(C_1)_{113}$ in the models for Refrigerant 113 is acceptable.

It is interesting to note that the extension of Vliet and Leppert's model to Refrigerant 113, as defined by equation (14), passes through the data at the highest flow rates tested. As indicated earlier, some rather liberal assumptions were made in using the $\bar{f}$ for water in the Refrigerant 113 derivation. However, there is some evidence that suggests that at the highest flow rates the Refrigerant 113 was, in fact, approaching the sheet region, thus suggesting that equation (14) may not be in serious error. This evidence is concerned with the rise rate of the vapor prior to and after separation from the heater.
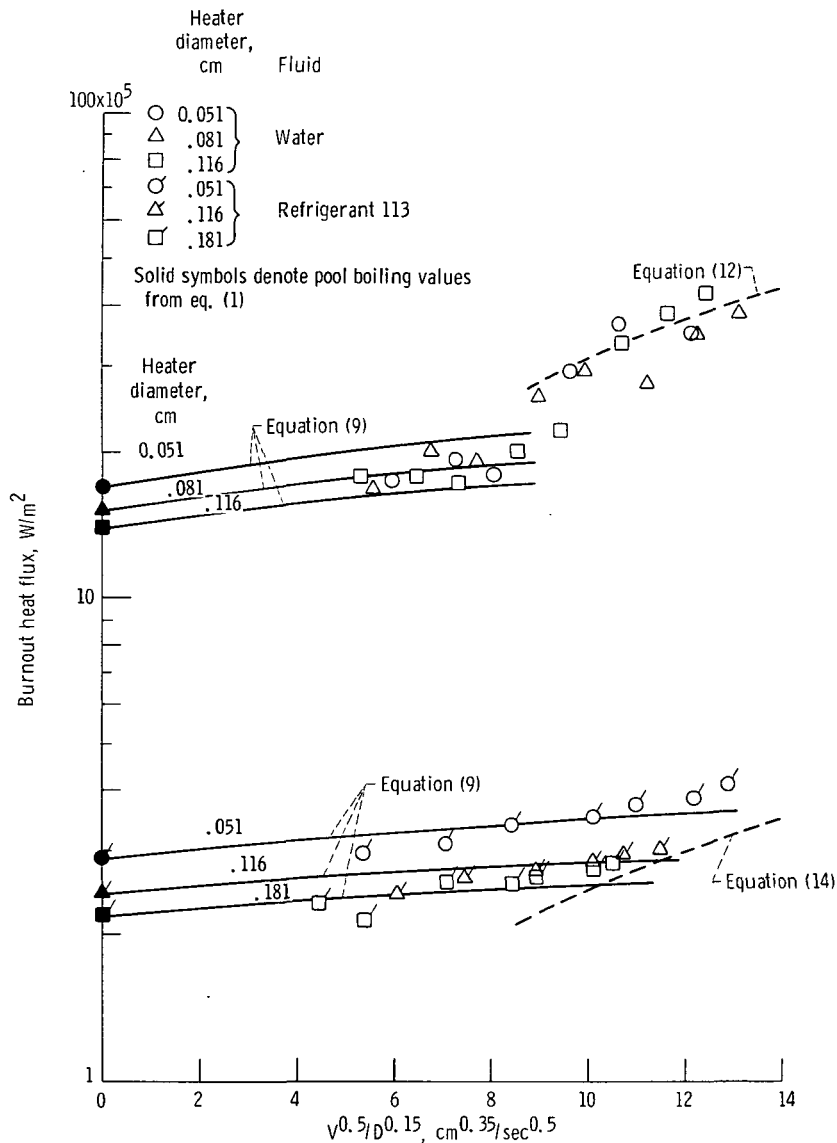
Figure 9. - Correlation of burnout heat flux data.

Qualitative information on the bubble rise rates was obtained at low and high flow rates for both water and Refrigerant 113. The low flow rate data (water, 14.5 cm/sec; Refrigerant 113, 20 cm/sec) indicates that the bubbles, under the influence of buoyancy, were moving faster than the liquid. This further substantiates under these conditions the use of the jet model which is highly dependent on buoyancy. At a high flow rate (water and Refrigerant 113, 60 cm/sec), the bubbles were moving at a rate equal to or slightly less than the liquid velocity. This suggests that the liquid flow was dominating the process and that the use of Vliet and Leppert's model is appropriate.

CONCLUSIONS

An investigation was conducted of the peak heat flux on cylindrical heaters in a saturated liquid in crossflow. The fluids used were water and Refrigerant 113. Average free stream velocity ranged from 10.1 to 81.1 centimeters per second. The following results were obtained:

1. The water data at high flow rates was adequately correlated by the prediction of Vliet and Leppert. However, at low flow rates the data's dependence on velocity deviated from this prediction.

2. The water data at low flow rates as well as all the Refrigerant 113 data were sucessfully predicted by a model based on a superposition of Lienhard's pool boiling prediction and a contribution due to single-phase forced convection.

This agreement between the data and the different mathematical models together with observations from the motion pictures suggest the following processes are controlling the peak heat flux in a forced convection situation:

1. At low flow rates the controlling process is the inability to remove vapor fast enough from the heater. Buoyancy and capillary forces are of prime importance. The instability of vapor jets and liquid columns dominates as is the case for pool boiling.

2. At higher flow rates the vapor removal patterns are altered from that at low flow rates and the controlling process becomes the deficiency of liquid in the two-phase mixture at the rear portion of the heater. The inertia of the flowing liquid dominates in determining the vapor motion.

Lewis Research Center,
    National Aeronautics and Space Administration,
        Cleveland, Ohio, October 11, 1973,
            502-24.

REFERENCES

1. Lienhard, John H.; and Dhir, Vijay K.: The Extended Hydrodynamic Theory of the Peak and Minimum Pool Boiling Heat Fluxes. NASA CR-2270, 1973.

2. Vliet, G. C.; and Leppert, G.: Critical Heat Flux for Nearly Saturated Water Flowing Normal to a Cylinder. Heat Transfer, vol. 86, no. 1, 1964, pp. 59-67.

3. McKee, Hugh R.: Forced Convection Boiling from a Cylinder Normal to the Flow. Ph. D. Thesis, Oklahoma State Univ., 1967.

4. Zuber, N.: Hydrodynamic Aspects of Boiling Heat Transfer. AEC Rep. AECU-4439, 1969.

5. Gambill, W. R.: Generalized Prediction of Burnout Heat Flux for Flowing, Subcooled, Wetting Liquids. Chem. Eng. Prog. Symp. Ser., vol. 59, n. 41, 1963, pp. 71-87.

6. Krieth, Frank: Principles of Heat Transfer., International Textbook Co., 1958.

7. Engelberg-Forster, Kurt; and Greif, R.: Heat Transfer to a Boiling Liquid-Mechanism and Correlations. J. Heat Transfer, vol. 81, no. 1, Feb. 1959, pp. 43-53.

8. Lippert, T. E.; and Dougall, R. S.: A Study of the Temperature Profiles Measured in the Thermal Sublayer of Water, Freon 113, and Methyl Alcohol During Boiling. J. Heat Transfer, vol. 90, no. 3, Aug. 1968, pp. 347-352.

"The aeronautical and space activities of the United States shall be conducted so as to contribute . . . to the expansion of human knowledge of phenomena in the atmosphere and space. The Administration shall provide for the widest practicable and appropriate dissemination of information concerning its activities and the results thereof."
—NATIONAL AERONAUTICS AND SPACE ACT OF 1958

NASA SCIENTIFIC AND TECHNICAL PUBLICATIONS

TECHNICAL REPORTS: Scientific and technical information considered important, complete, and a lasting contribution to existing knowledge.

TECHNICAL NOTES: Information less broad in scope but nevertheless of importance as a contribution to existing knowledge.

TECHNICAL MEMORANDUMS: Information receiving limited distribution because of preliminary data, security classification, or other reasons. Also includes conference proceedings with either limited or unlimited distribution.

CONTRACTOR REPORTS: Scientific and technical information generated under a NASA contract or grant and considered an important contribution to existing knowledge.

TECHNICAL TRANSLATIONS: Information published in a foreign language considered to merit NASA distribution in English.

SPECIAL PUBLICATIONS: Information derived from or of value to NASA activities. Publications include final reports of major projects, monographs, data compilations, handbooks, sourcebooks, and special bibliographies.

TECHNOLOGY UTILIZATION PUBLICATIONS: Information on technology used by NASA that may be of particular interest in commercial and other non-aerospace applications. Publications include Tech Briefs, Technology Utilization Reports and Technology Surveys.

Details on the availability of these publications may be obtained from:

SCIENTIFIC AND TECHNICAL INFORMATION OFFICE

NATIONAL AERONAUTICS AND SPACE ADMINISTRATION
Washington, D.C. 20546